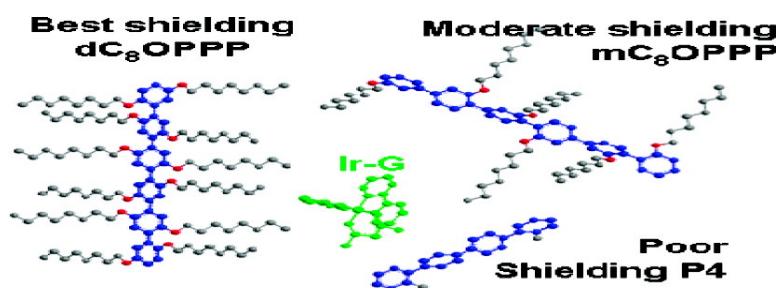


Effective Shielding of Triplet Energy Transfer to Conjugated Polymer by Its Dense Side Chains from Phosphor Dopant for Highly Efficient Electrophosphorescence

Szu-Po Huang, Tzu-Hao Jen, Yen-Chun Chen, An-En Hsiao, Shu-Hui Yin, Hsiang-Yun Chen, and Show-An Chen

J. Am. Chem. Soc., **2008**, 130 (14), 4699-4707 • DOI: 10.1021/ja076413i

Downloaded from <http://pubs.acs.org> on February 8, 2009



More About This Article

Additional resources and features associated with this article are available within the HTML version:

- Supporting Information
- Links to the 1 articles that cite this article, as of the time of this article download
- Access to high resolution figures
- Links to articles and content related to this article
- Copyright permission to reproduce figures and/or text from this article

[View the Full Text HTML](#)



Effective Shielding of Triplet Energy Transfer to Conjugated Polymer by Its Dense Side Chains from Phosphor Dopant for Highly Efficient Electrophosphorescence

Szu-Po Huang, Tzu-Hao Jen, Yen-Chun Chen, An-En Hsiao, Shu-Hui Yin, Hsiang-Yun Chen, and Show-An Chen*

Chemical Engineering Department, National Tsing-Hua University, Hsinchu, 30041, Taiwan, R.O.C.

Received August 26, 2007; E-mail: sachen@che.nthu.edu.tw

Abstract: To examine the quenching of a triplet exciton by low triplet energy (E_T) polymer hosts with different chain configurations for high E_T phosphor guests, the quenching rate constant measurements were carried out and analyzed by the standard Stern–Volmer equation. We found that an effective shielding of triplet energy transfer from a high E_T phosphor guest to a low E_T polymer host is possible upon introducing dense side chains to the polymer to block direct contact from the guest such that the possibility of Dexter energy transfer between them is reduced to a minimum. Together with energy level matching to allow charge trapping on the guest, high device efficiency can be achieved. The extent of shielding for the systems of phenylene-based conjugated structures from iridium complexes follows the sequence di-substituted (octoxyl chain) in the para position (dC₈OPPP) is greater than monosubstituted (mC₈OPPP) and the PPPs with longer side chains are much higher than a phenylene tetramer (P4) with two short methyl groups. Further, capping the dialkoxy-substituents with a carbazole (Cz) moiety (CzPPP) provides enhanced extent of shielding. Excellent device efficiency of 30 cd/A (8.25%) for a green electrophosphorescent device can be achieved with CzPPP as a host, which is higher than that of dC₈OPPP as host (15 cd/A). The efficiency is higher than those of high E_T conjugated polymers, poly(3,6-carbazole) derivatives, as hosts (23 cd/A). This observation suggests a new route for molecular design of electroluminescent polymers as a host for a phosphorescent dopant.

Introduction

In organic and polymeric light emitting diodes (LEDs), holes and electrons injected from the anode and cathode can recombine to yield singlet and triplet excitons at a population ratio of 1:3 according to quantum statistics and some experiments,¹ to which the ratio in polymer LED remains in debate.² For a purely fluorescent device, only singlet is emissive and most of the energy is wasted by a nonemissive triplet. By doping with heavy-metal complexes as guests in small molecules or polymers as hosts,³ both singlet and triplet excitons can be harvested and consequently the internal quantum efficiency is able to be promoted toward 100%.^{3d–f} The reason is that the heavy-metal complexes can induce strong spin–orbital coupling and thus promote an efficient intersystem crossing (ISC) from its singlet excited state, eventually to the lowest-energy triplet excited state of the guest followed by relaxation to the ground state via phosphorescence at room temperature. In general, for such host/guest systems, the singlet excitons of heavy-metal complexes

are produced by Förster (long-range dipole–dipole induced)³ energy transfer from the host or by charge trapping (CT)^{1a,3h} on itself, and triplet excitons are generated by Dexter (short-range electron exchange)³ transfer from the host or by CT on itself. However, it is not the general case that triplet energy transfer is via short-range Dexter transfer. It was found recently that triplet energy transfer between two iridium (Ir) complex molecules can also take place via long-range Förster transfer⁴ and its transfer rate is dependent on intermolecular distance.^{4a} The reason is that large spin-orbital coupling associated with a heavy metal (e.g., Ir) causes formally spin-forbidden $S_0 \rightarrow T_1$ absorption to be allowed. Due to the larger extinction coefficient

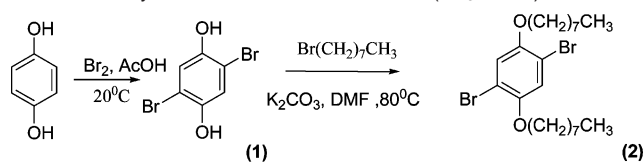
- (1) (a) Baldo, M. A.; O'Brien, D. F.; Thompson, M. E.; Forrest, S. R. *Phys. Rev. B* **1999**, *60*, 14422–14428. (b) Wilson, J. S.; Dhoot, A. S.; Seeley, A.; Khan, M. S.; Kohler, A.; Friend, R. H. *Nature* **2001**, *413*, 828–831. (c) Segal, M.; Baldo, M. A.; Holmes, R. J.; Forrest, S. R.; Soos, Z. G. *Phys. Rev. B* **2003**, *68*, 75211. (2) (a) Wohlgenannt, M.; Tandon, K.; Mazumdar, S.; Ramasesha, S.; Vardeny, Z. V. *Nature* **2001**, *409*, 494–497. (b) Rothe, C.; King, S. M.; Monkman, A. P. *Phys. Rev. Lett.* **2006**, *97*, 76602.

- (3) (a) Baldo, M. A.; O'Brien, D. F.; You, Y.; Shoustikov, A.; Sibley, S.; Thompson, M. E.; Forrest, S. R. *Nature* **1998**, *395*, 151–154. (b) Lamansky, S.; Djurovich, P.; Murphy, D.; Abdol-Razzaq, F.; Lee, H. E.; Adachi, C.; Burrows, P. E.; Forrest, S. R.; Thompson, M. E. *J. Am. Chem. Soc.* **2001**, *123*, 4304–4312. (c) Sudhakar, M.; Djurovich, P. I.; Hogen-Esch, T. E.; Thompson, M. E. *J. Am. Chem. Soc.* **2003**, *125*, 7796–7797. (d) Kawamura, Y.; Goushi, K.; Brooks, J.; Brown, J. J.; Sasabe, H.; Adachi, C. *Appl. Phys. Lett.* **2005**, *86*, 71104. (e) Adachi, C.; Baldo, M. A.; Thompson, M. E.; Forrest, S. R. *J. Appl. Phys.* **2001**, *90*, 5048–5051. (f) Sun, Y. R.; Giebink, N. C.; Kanno, H.; Ma, B. W.; Thompson, M. E.; Forrest, S. R. *Nature* **2006**, *440*, 908–912. (g) Chen, F. C.; Chang, S. C.; He, G. F.; Pyo, S.; Yang, Y.; Kurotaki, M.; Kido, J. *J. Polym. Sci., Part B: Polym. Phys.* **2003**, *41*, 2681–2690. (h) Baldo, M. A.; Forrest, S. R. *Phys. Rev. B* **2000**, *62*, 10958–10966. (i) Turro, N. J. *Modern Molecular Photochemistry*; University Science Books: Sausalito, CA, 1991; pp 311–316. (4) (a) Namdas, E. B.; Ruseckas, A.; Samuel, I. D. W.; Lo, S. C.; Burn, P. L. *Appl. Phys. Lett.* **2005**, *86*, 91104. (b) Wasserberg, D.; Meskers, S. C. J.; Janssen, R. A. J. *J. Phys. Chem. A* **2007**, *111*, 1381–1388. (c) Rothe, C.; King, S.; Monkman, A. *Nat. Mater.* **2006**, *5*, 463–466.

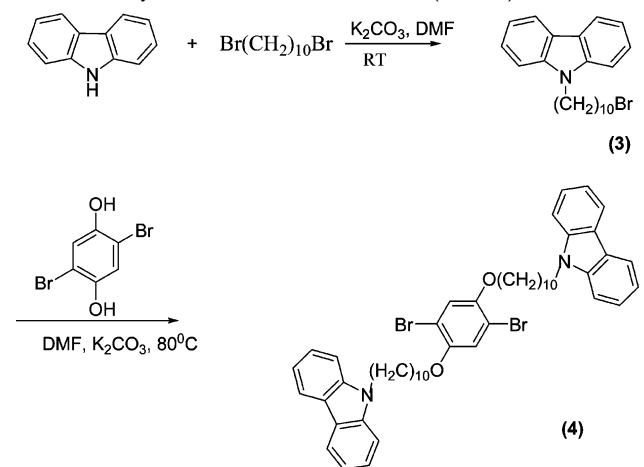
(ϵ) of the S–T transition caused by this heavy atom effect, the triplet energy transfer between two Ir-complex molecules can take place via the long-range Förster mechanism. However, in the case of Ir complexes doping into polymers (or small molecules), the small ϵ of the S–T transition of polymers (or small molecules) without heavy metal perturbation, the triplet energy transfer is mainly via the short-range Dexter mechanism and negligible via the long-range Förster mechanism.

In order to confine triplet excitons on a phosphor guest, a host material with a triplet energy level (E_T) higher than that of the phosphor guest is intuitively required as a significant quencher of triplet excitons by a low E_T host for a high E_T guests can occur, as evidenced by the Stern–Volmer analysis for the system of various Ir complexes ranging from a blue to red emission with tris(9,9-dimethylfluorene) (F3) as the phosphor quencher.^{3c} High E_T conjugated polymers such as poly(3,6-carbazole) derivatives, P(3,6-Cz)'s with $E_T \approx 2.6$ eV,⁵ have been prepared by limiting the conjugation length of the backbone to biphenyl. Upon doping with a green emitting Ir complex (Ir–G, (bis(2-phenylpyridinato-N,C^{2'})iridium(acetylacetonate))), the excellent performance with a maximum luminous efficiency (η) of about 23 cd/A, equivalent to an external quantum efficiency (η_{ext}) of about 6.6%, was obtained. The common blue-emitting polymers,⁶ polyfluorenes (PFs) ($E_T = 2.18$ eV) and poly(*p*-phenylene)s (PPPs) ($E_T = 2.27$ eV), are usually low in E_T and expected to be not suitable for use as hosts for high E_T guests, e.g., Ir–G. As stated above, since triplet energy transfer between a conjugated polymer host and phosphor guest is dominated via electron exchange (requiring a close contact within 15 Å),⁷ some efforts^{8a,b} have been attempted recently to reduce the back triplet energy transfer from guest to host by increasing the distance between their triplet centers. For the case with similar E_T values for the polymer host and iridium guest, the device η_{ext} can be improved from 1.1% to 2.0%^{8a} by grafting red-emitting (btp)₂Ir(acac) ($E_T = 2.0$ eV) with the spacer, $-(\text{CH}_2)_8-$, as the side chain^{8a,c} on poly(9,9'-dioctyl-fluorene) (PFO, $E_T = 2.18$ eV) as compared to that without the spacer. Alternatively, introducing a bulky *tert*-butyl group as a side group on each ring in the ligands of green-emitting Ir(ppy)₃ ($E_T = 2.4$ eV) has also been found to promote device η_{ext} from 0.1 to 0.4%^{8b} when used as a dopant for poly(9,9'-spirobifluorene) ($E_T = 2.18$ eV) relative to the system with the same dopant but without such modification, which reflects a reduced triplet energy transfer back to the host. However, the chance for Ir-complex molecules to contact with main chains for both cases still remains high, since the Ir complexes on a side chain can still be able to be in contact with the polymer backbone nearby and the distance from the hydrogen atom of the *tert*-butyl group to the center Ir atom is within 10 Å (within the effective distance for Dexter energy transfer). In addition, trace host emission under electrical excitation can still be observed in both cases.

Scheme 1. Synthetic Route for Monomer 2 (dC₈OPPP)



Scheme 2. Synthetic Route for Monomer 4 (CzPPP)



Hence, the efficiency of the green electrophosphorescent devices is still low for the use of low E_T hosts (PFs^{3g,8b} and PPPs^{9a,b}) as compared to that with the high E_T hosts, P(3,6-Cz)'s⁵ and PVK^{9c–e} (the measured value $E_T = 2.91$ eV as shown in the Supporting Information (SI), which is identical to that reported in ref 10). More importantly, a design route for a low E_T polymer as an effective host for a high E_T guest still remains unclear.

Here, we demonstrate that an effective shielding of triplet energy transfer from a high E_T phosphor guest to a low E_T polymer host is possible upon introducing dense side chains to the polymer to block direct contact from the guest such that the possibility of Dexter energy transfer between them is reduced to a minimum. Together with energy levels matching to allow charge trapping on the guest, high device efficiency can be achieved. The system investigated is dialkoxy-substituted PPP (dC₈OPPP) ($E_T = 2.31$ eV) as the host and Ir–G ($E_T = 2.41$ eV) as the guest, which gives a high device η of 15 cd/A (4.12%). With further capping of the dialkoxy-substituents with a carbazole (Cz) moiety (CzPPP), the device η is further promoted to 30 cd/A (8.25%). The further promoted efficiency can be attributed to better chemical compatibility between the host and guest provided by the Cz. This observation suggests a new route for molecular design of electroluminescent polymers as a host for a phosphorescent dopant.

Experimental Section

Synthesis of Monomers and Polymers. The polymers (mC₈OPPP, dC₈OPPP, CzPPP, PFO, and CzPF) were synthesized by a Yamamoto polymerization method, and mC₈OPPP¹¹ and PFs^{8c} syntheses were

- (5) (a) van Dijken, A.; Bastiaansen, J.; Kiggen, N. M. M.; Langeveld, B. M. W.; Rothe, C.; Monkman, A.; Bach, I.; Stossel, P.; Brunner, K. *J. Am. Chem. Soc.* **2004**, *126*, 7718–7727. (b) Chen, Y. C.; Huang, G. S.; Hsiao, C. C.; Chen, S. A. *J. Am. Chem. Soc.* **2006**, *128*, 8549–8558.
- (6) Hertel, D.; Setayesh, S.; Nothofer, H. G.; Scherf, U.; Mullen, K.; Bassler, H. *Adv. Mater.* **2001**, *13*, 65–70.
- (7) Turro, N. J. *Modern Molecular Photochemistry*; University Science Books: Sausalito, CA, 1991; pp 328–330.
- (8) (a) Evans, N. R.; Devi, L. S.; Mak, C. S. K.; Watkins, S. E.; Pascu, S. I.; Kohler, A.; Friend, R. H.; Williams, C. K.; Holmes, A. B. *J. Am. Chem. Soc.* **2006**, *128*, 6647–6656. (b) King, S. M.; Al-Attar, H. A.; Evans, R. J.; Congreve, A.; Beeby, A.; Monkman, A. P. *Adv. Funct. Mater.* **2006**, *16*, 1043–1050. (c) Chen, X. W.; Liao, J. L.; Liang, Y. M.; Ahmed, M. O.; Tseng, H. E.; Chen, S. A. *J. Am. Chem. Soc.* **2003**, *125*, 636–637.

- (9) (a) Zhu, W. G.; Mo, Y. Q.; Yuan, M.; Yang, W.; Cao, Y. *Appl. Phys. Lett.* **2002**, *80*, 2045–2047. (b) Zhu, W. G.; Liu, C. Z.; Su, L. J.; Yang, W.; Yuan, M.; Cao, Y. *J. Mater. Chem.* **2003**, *13*, 50–55. (c) Suzuki, M.; Tokito, S.; Sato, F.; Igarashi, T.; Kondo, K.; Koyama, T.; Yamaguchi, T. *Appl. Phys. Lett.* **2005**, *86*, 103507. (d) Kim, T. H.; Yoo, D. H.; Park, J. H.; Park, O. O.; Yu, J. W.; Kim, J. K. *Appl. Phys. Lett.* **2005**, *86*, 171108. (e) Choulis, S. A.; Mathai, M. K.; Choong, V. E.; So, F. *Appl. Phys. Lett.* **2006**, *88*, 203502.
- (10) (a) Burkhart, R. D.; Chakraborty, D. K. *J. Phys. Chem.* **1990**, *94*, 4143–4147. (b) Pina, J.; de Melo, J. S.; Burrows, H. D.; Monkman, A. P.; Navaratnam, S. *Chem. Phys. Lett.* **2004**, *400*, 441–445.

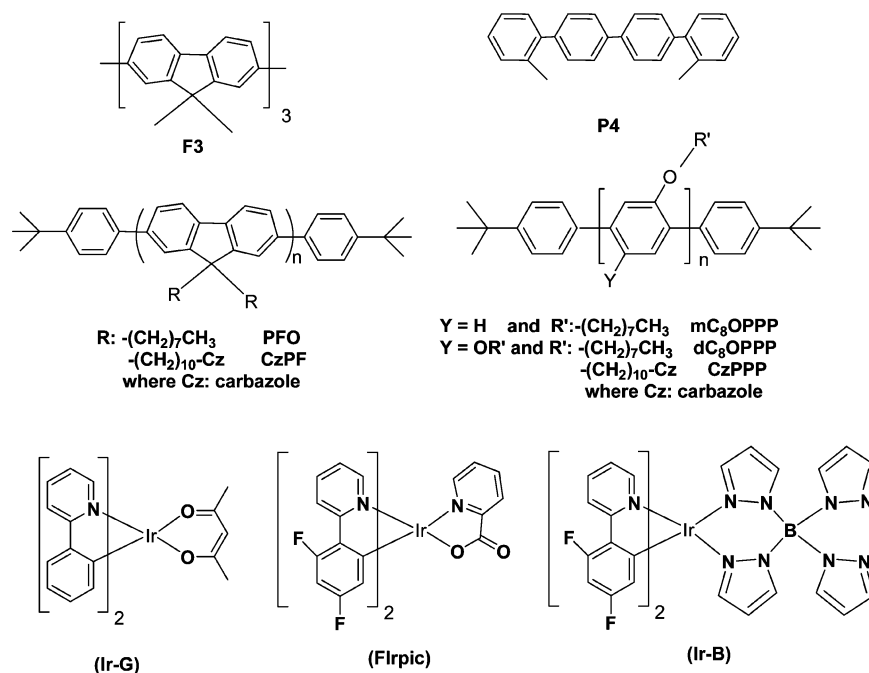


Figure 1. Chemical structures of F3, P4, PFO, CzPF, mC₈OPPP, dC₈OPPP, and CzPPP as hosts (quenchers in Stern–Volmer analysis) and Ir–G, Flrpic, and Ir–B as guests.

carried out according to our previous reports. The reaction routes for monomers are given in Schemes 1 and 2. The detailed synthetic procedures for the monomers and polymers are described in the SI.

Instrumentation. Ultraviolet–visible (UV–vis), photoluminescence (PL), photoexcitation (PLE), electroluminescence (EL), phosphorescence, gel permeation chromatography (GPC), scanning probe microscopy (SPM), the film thickness monitor and power supplier as well as luminance meter for measurements of device performance are also described in detail in the SI.

Device Fabrication and General Instrumentation. Indium–tin oxide (ITO) glass plates were treated with oxygen plasma and then coated with a CF_x thin film as a hole injection layer¹² by plasma polymerization of CF₃H in a chamber of parallel electrode type equipped with a 13.56 MHz radio frequency (rf) power generator. Its thickness is about 2 nm as estimated using an ellipsometric spectrometer (from Jobin Yvon). On top of it, a thin layer (emitting polymer layer, ca. 100 nm) of emitting polymer was spin-cast from its solution (10 mg/mL) in THF. The 1,3,5-tri(phenyl-2-benzimidazolyl)-benzene (TPBI) layer (30 nm), which was used as a hole/exciton blocking layer, was grown by thermal evaporation in a vacuum thermal evaporator through a shadow mask at a vacuum of 2×10^{-6} Torr. Finally, thin layers of CsF (about 1 nm) and then calcium (about 5 nm) covered with a layer of aluminum as the cathode for the bipolar device was deposited in a vacuum thermal evaporator through a shadow mask at a pressure of less than 2×10^{-6} Torr. The active area of the diode is about 10 mm². A surface profiler (Tencor P-10) was used for determining polymer film thickness.

Results and Discussion

Photophysical Properties (UV–vis Absorption, Photoluminescence). The chemical structures of mC₈OPPP, dC₈OPPP,

and CzPPP are shown in Figure 1, and their UV–vis absorption and photoluminescence (PL) spectra in THF solutions and as thin solid films along with the absorption spectrum of carbazole in THF are shown in Figure 2. The absorption maxima of dC₈OPPP and mC₈OPPP in THF are 337 and 335 nm, respectively. However, the absorption peaks of CzPPP in THF at 261, 294, 332, and 345 nm show similar features to those of Cz in THF, causing identification of the absorption (at 332 or 345 nm) for the polymer backbone or pendant Cz to be difficult. The absorption peaks of PPPs in thin solid films (Figure 2b) show a red-shift by about 2 nm as compared with their corresponding peaks in solutions except for dC₈OPPP (4 nm red-shift). The PL spectra of all the PPPs in THF show the same emission maxima at 399 nm regardless of the difference in side groups. However, the emission maxima in thin solid films show red-shifts to 400, 411, and 442 nm for CzPPP, mC₈OPPP, and dC₈OPPP, respectively, as compared with the corresponding peaks in solutions (all at 399 nm). The large red-shifts of emission maxima for mC₈OPPP and dC₈OPPP could be attributed to a presence of aggregates which emit a lower energy light¹³ or an increase of conjugation length in films relative to that in solutions.

Figure 3a shows the UV–vis absorption spectrum of Ir–G and PL emission spectra of PFs and PPPs in THF solutions. The Förster energy transfer from the hosts to guest is expected to occur due to the good spectral overlap between the absorption of metal-to-ligand charge-transfer bands (410–460 nm) of Ir–G^{3b} and the emission spectra of the polymers. However, the PL spectrum of a 8 wt % Ir–G doped PFO film does not show an Ir–G emission (peak maximum at 518 nm, Figure 3b) at all, resulting from triplet excitons in Ir–G being significantly quenched by the lower E_T PFO.^{3g} The extent of quenching is reduced as CzPF is used as the host as reflected by a weak emission from Ir–G relative to the emission from the host. Both

(11) Chen, S. A.; Chao, C. I. *Synth. Met.* **1996**, *79*, 93–96.
 (12) (a) Hsiao, C. C.; Chang, C. H.; Jen, T. H.; Hung, M. C.; Chen, S. A. *Appl. Phys. Lett.* **2006**, *88*, 33512. (b) Hsiao, C. C.; Chang, C. H.; Lu, H. H.; Chen, S. A. *Org. Electron.* **2007**, *8*, 343–348. (c) Hung, L. S.; Zheng, L. R.; Mason, M. G. *Appl. Phys. Lett.* **2001**, *78*, 673–675. (d) Tong, S. W.; Lee, C. S.; Lifshitz, Y.; Gao, D. Q.; Lee, S. T. *Appl. Phys. Lett.* **2004**, *84*, 4032–4034. (e) Tang, J. X.; Li, Y. Q.; Hung, L. S.; Lee, C. S. *Appl. Phys. Lett.* **2004**, *84*, 73–75. (f) Tang, J. X.; Li, Y. Q.; Zheng, L. R.; Hung, L. S. *J. Appl. Phys.* **2004**, *95*, 4397–4403.

(13) (a) Peng, K. Y.; Chen, S. A.; Fann, W. S. *J. Am. Chem. Soc.* **2001**, *123*, 11388–11397. (b) Peng, K. Y.; Chen, S. A.; Fann, W. S.; Chen, S. H.; Su, A. C. *J. Phys. Chem. B* **2005**, *109*, 9368–9373.

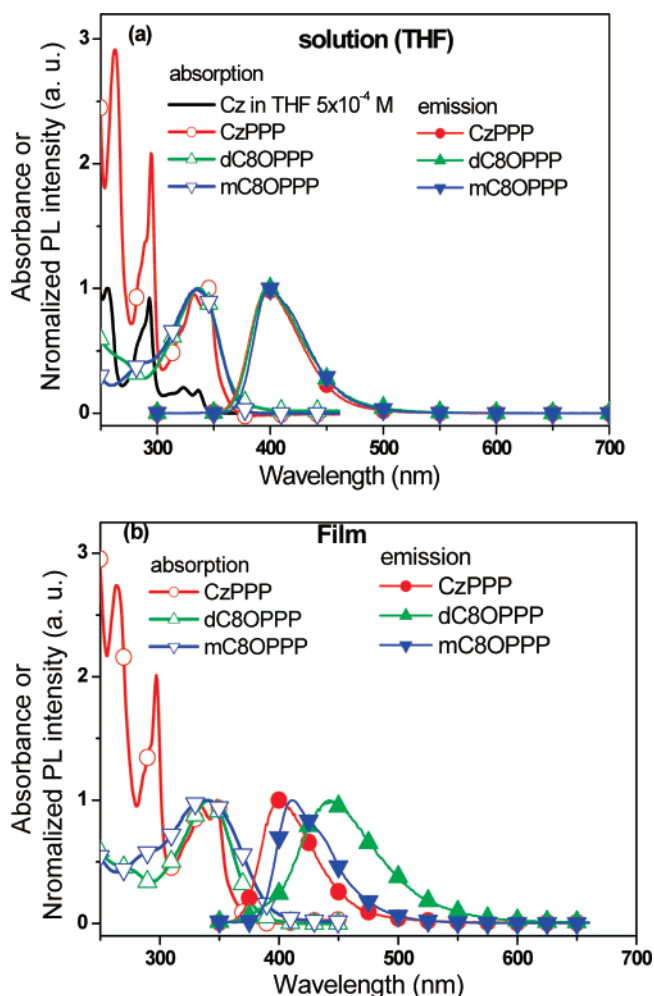


Figure 2. UV-vis absorption and normalized PL emission spectra of PPPs (a) in THF solution and (b) as thin solid films. The absorption spectrum of carbazole is also provided in (a).

cases reveal the predominant host emission (the corresponding mol % of Ir-G doping for PFO and CzPF based on their repeat units are 5 mol % and 10 mol %, respectively). Surprisingly, the predominant Ir-G emissions are observed for the cases with PPPs as hosts also at the 8 wt % doping level (the corresponding mol % of Ir-G doping for mC₈OPPP, dC₈OPPP, and CzPPP based on their repeat units are 2.7 mol %, 4.4 mol %, and 9.5 mol %, respectively), in which no host emission for CzPPP, a weak host emission at 442 nm for dC₈OPPP, and a moderate host emission at 411 nm for mC₈OPPP are observed even though the PPPs have a lower E_T (E_T of CzPPP = 2.39 eV, E_T of dC₈OPPP = 2.31 eV, and E_T of mC₈OPPP = 2.3 eV) than Ir-G (2.41 eV).

One may argue that Ir-G emission in CzPF may be due to relative high mol % (10%) Ir-G doping concentration as compared to that of PFO (5%). Therefore, the emission spectra of PFs doped with 10 mol % Ir-G and PPPs doped with 4.4 mol % are also provided in Figure 3c to clarify this point. The dopant concentrations of 10 mol % Ir-G for PFs are equal to those of 16 and 8 wt % for PFO and CzPF, respectively, and those of 4.4 mol % for PPPs are equal to those of 13, 8, and 3.7 wt % for mC₈OPPP, dC₈OPPP, and CzPPP, respectively. As compared with Figure 3b (8 wt % Ir-G doped polymers), only a very weak CzPPP emission for 3.7 wt % Ir-G doped CzPPP and a drop of mC₈OPPP emission for 13 wt % Ir-G

doped mC₈OPPP are observed. However, as shown in Figure 3c, the relative host/guest intensities between Ir-G doped PFs as well as PPPs exhibit similar trends in Figure 3b. Hence, we can rule out the doping level effect (wt % or mol %) that might lead to a variation in relative host/guest intensities between Ir-G and host in the range of doping level investigated. But the other possible factors can also affect the spectra in the solid state, such as a shielding effect of triplet energy transfer to conjugated polymers by configuration of their side chains, E_T of host, and chemical compatibility between host and guest,^{3g,9d,14} as will be discussed later.

Shielding Effect Provided by Side Chains: Quantitative Measurements via Stern-Volmer Analysis for Quenching Rate Constants. In order to examine more specifically the quenching of triplet excitons in phosphor dopants by low E_T polymer hosts with different chain configurations, F3, P4, PFs, and PPPs as triplet quenchers for Ir-G, Firpic, and Ir-B (their chemical structures are shown in Figure 1) were measured and analyzed by the standard Stern-Volmer equation^{3c} (see SI for detail). The quenching analysis involves two parts: (a) a fluorene-based series containing F3 with a short side chain (methyl) and PFs with long side chains and (b) a phenylene-based series containing P4 with a short side chain (methyl) and PPPs with long side chains. The results of the Stern-Volmer quenching analysis along with the E_T 's of the materials investigated are shown in Table 1. Due to the variations in E_T 's of the materials (Table 1 and SI), the E_T difference between guest and host ($\Delta E_T = E_{T,\text{guest}} - E_{T,\text{host}}$) is plotted versus the quenching rate constant (K_{qsv}) as shown in Figure 4, though the K_{qsv} is influenced not only by ΔE_T but also by several other parameters, like steric hindrance.^{8a,b}

For fluorene-based F3 and PFs as quenchers for Ir-G, the K_{qsv} 's of F3, PFO, and CzPF are 1.14×10^9 , 2.06×10^8 , and 1.76×10^8 (Ms)⁻¹ (Table 1), respectively. The K_{qsv} 's of PFO and CzPF are lower than that of F3 by 1 order of magnitude, though the E_T of F3 is significantly higher than those of PFs by 0.13 eV. This would indicate that doping the Ir complex into PFO instead of grafting onto the PF backbone spaced by $-(\text{CH}_2)_8$ ^{-8a} can also reduce triplet energy transfer to the host and that side chains do provide a significant shielding effect for quenching.

For phenylene-based P4 and PPPs as quenchers, the K_{qsv} of P4 for Ir-G is lower than those of PPPs by a factor of 2–15 (Table 1) due to the fact that the triplet energy transfer from P4 to Ir-G is energetically unfavorable ($\Delta E_T < 0$) leading to the lowest K_{qsv} . Interestingly, the K_{qsv} 's of PPPs for Ir-B are lower than those of the corresponding PPPs for Firpic by a factor of 1.3–2.1 even though the energy gaps are larger by about 0.1 eV. It appears that the K_{qsv} is also influenced by the steric hindrance provided by the larger substituents at the Ir-core of Ir-B.^{8b} In general, as $\Delta E_T > 0$, the K_{qsv} 's of P4 and PPPs for the same Ir complex follow the sequence P4 > mC₈OPPP > dC₈OPPP > CzPPP even though the E_T of P4 is higher than

(14) Noh, Y. Y.; Lee, C. L.; Kim, J. J.; Yase, K. *J. Chem. Phys.* **2003**, *118*, 2853–2864.

(15) (a) Adachi, C.; Kwong, R. C.; Djurovich, P.; Adamovich, V.; Baldo, M. A.; Thompson, M. E.; Forrest, S. R. *Appl. Phys. Lett.* **2001**, *79*, 2082–2084. (b) Holmes, R. J.; D'Andrade, B. W.; Forrest, S. R.; Ren, X.; Li, J.; Thompson, M. E. *Appl. Phys. Lett.* **2003**, *83*, 3818–3820. (c) Chi, C. Y.; Im, C.; Wegner, G. *J. Chem. Phys.* **2006**, *124*, 24907. (d) Allen, B. D.; Benniston, A. C.; Harriman, A.; Llarena, I.; Sams, C. A. *J. Phys. Chem. A* **2007**, *111*, 2641–2649. (e) Lafolet, F.; Welter, S.; Popovic, Z.; De Cola, L. *J. Mater. Chem.* **2005**, *15*, 2820–2828.

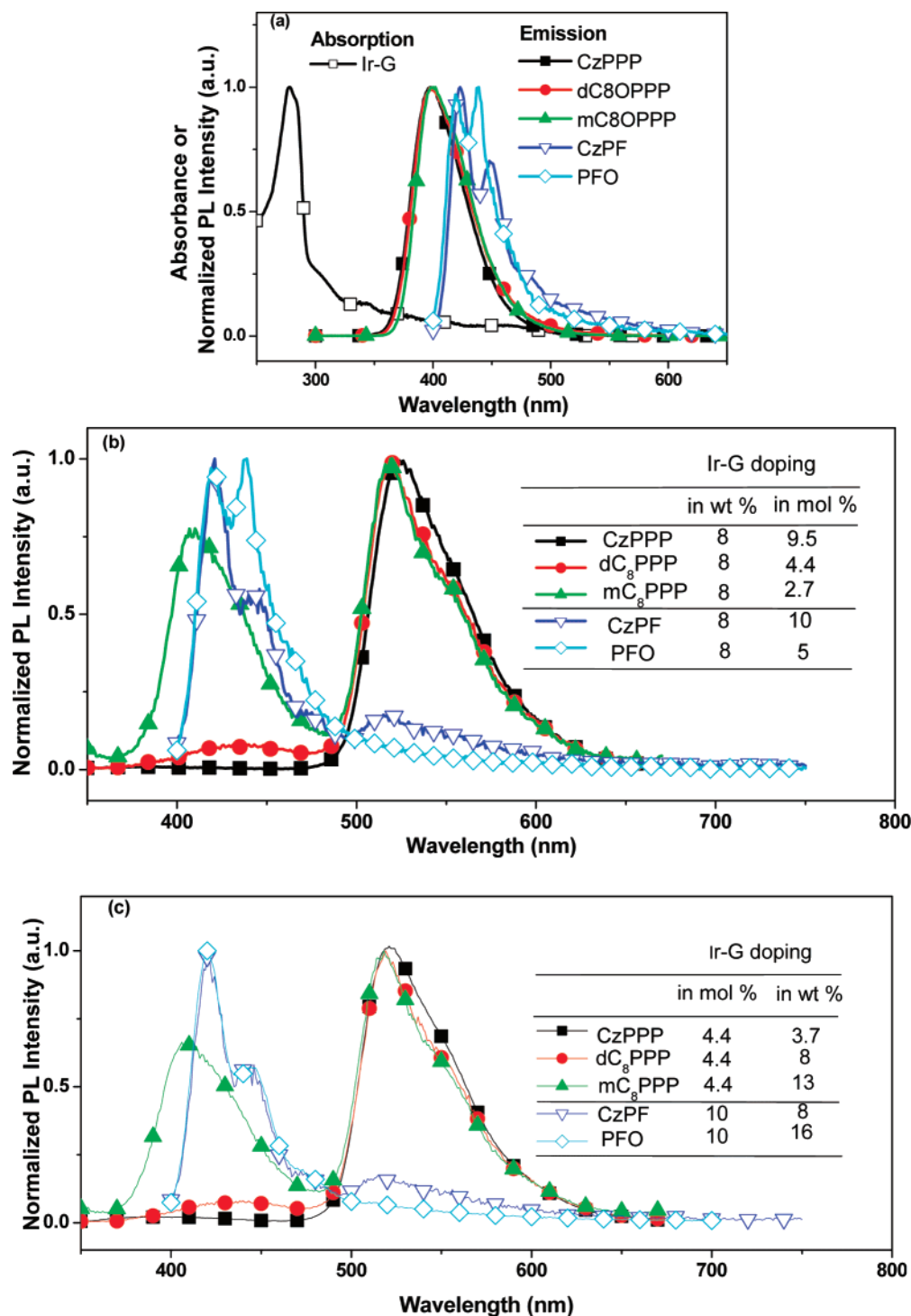


Figure 3. (a) UV-vis absorption spectrum of Ir-G and normalized PL emission spectra of PFs and PPPs in THF solutions. (b) Normalized PL spectra of PFs and PPPs as thin films doped with 8 wt % Ir-G and (c) normalized PL spectra of PFs as thin film doped with 10 mol % Ir-G and PPPs as thin film doped with 4.4 mol % Ir-G, respectively. The inserted table on the right side in Figure 3b is the wt % and corresponding mol % Ir-complex doping concentrations, and that in Figure 3c is the mol % and corresponding wt % Ir-complex doping concentrations. The mol % is calculated based on their repeat unit of the polymer (PFs are excited at 388 nm, and PPPs are excited at 340 nm).

that of all PPPs (Table 1 and Figure 4). This reflects that the shielding provided by the side chains could overcompensate for the difference in E_T , and the extent of shielding by the disubstitution is significantly higher than that of the monosubstitution. The reason is that the two side chains of dC₈OPPP are schematically nearly orthogonal¹⁶ with those of its neighboring repeat unit; thus the available space is so crowded for an Ir-G molecule to insert into, and the chance for the aromatic

rings of the ligands to be in contact with the main chain is only possible at a specific molecular orientation (Figure S5). For mC₈OPPP, there is only one side chain per aromatic ring, leading to a sufficiently large space available for an Ir-G molecule to be accommodated at any orientation. Furthermore, K_{qsv} 's

(16) (a) Park, K. C.; Dodd, L. R.; Levon, K.; Kwei, T. K. *Macromolecules* **1996**, *29*, 7149–7154. (b) Pasco, S. T.; Baker, G. L. *Synth. Met.* **1997**, *84*, 275–276.

Table 1. Data for the Stern–Volmer Quenching Analysis along with the Triplet Energies^a of the Materials Investigated

iridium complex (triplet energy)	quencher (triplet energy)	$\Delta E_T =$	
		$E_{T, \text{guest}} - E_{T, \text{host}}$ (eV)	K_{qsv}^b ($\text{M}^{-1} \text{s}^{-1}$)
Ir–G ($E_T = 2.41 \text{ eV}$) ^c	F3 ($E_T = 2.31 \text{ eV}$) ^f	0.10	1.14×10^9
	PFO ($E_T = 2.18 \text{ eV}$)	0.23	2.06×10^8
	CzPF ($E_T = 2.18 \text{ eV}$)	0.23	1.76×10^8
	P4 ($E_T = 2.44 \text{ eV}$) ^g	−0.03	6.60×10^5
	mC ₈ OPPP ($E_T = 2.3 \text{ eV}$)	0.11	1.00×10^7
dC ₈ OPPP ($E_T = 2.31 \text{ eV}$)		0.10	3.75×10^6
	CzPPP ($E_T = 2.39 \text{ eV}$)	0.02	1.44×10^6
Flrpic ($E_T = 2.62 \text{ eV}$) ^d	F3	0.31	2.74×10^9
	P4	0.18	1.83×10^8
	mC ₈ OPPP	0.32	9.24×10^7
	dC ₈ OPPP	0.31	3.48×10^7
	CzPPP	0.23	1.92×10^7
Ir–B ($E_T = 2.72 \text{ eV}$) ^e	P4	0.28	2.88×10^8
	mC ₈ OPPP	0.42	6.49×10^7
	dC ₈ OPPP	0.41	2.71×10^7
	CzPPP	0.33	9.22×10^6

^a The maximum of the first vibronic transition ($T_1^{\nu=0} \rightarrow S_0^{\nu=0}$) of the phosphorescence spectrum is taken as E_T (see the section “delay luminescence” in SI). ^b The Stern–Volmer equation $\tau_0/\tau = \tau_0 K_{\text{qsv}}[Q] + 1$ was used, where τ and τ_0 are lifetimes of the phosphor with and without the quencher, K_{qsv} is the Stern–Volmer quenching rate constant, and $[Q]$ is the concentration of the quencher. ^c Reference 3b. ^d Reference 15a. ^e Reference 15b. ^f Reference 15c. ^g Reference 15d and e.

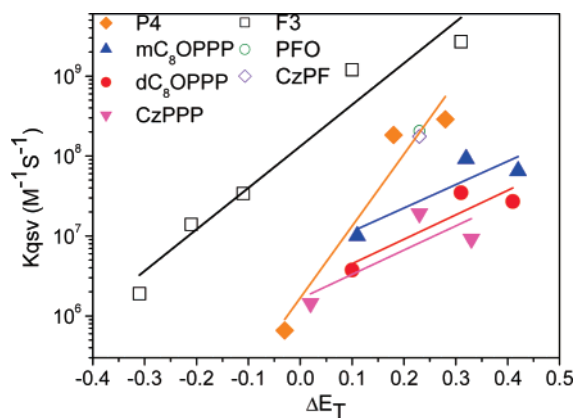


Figure 4. Triplet energy difference between guest and host ($\Delta E_T = E_{T, \text{guest}} - E_{T, \text{host}}$) versus quenching rate constant K_{qsv} . The K_{qsv} data of F3 for various Ir complexes are taken from ref 3c (see SI for details). The solid lines are for a visual guide.

become even smaller by the incorporation of Cz on the end of each side chain for CzPPP and CzPF relative to their analogues dC₈OPPP and PFO, respectively. This is mainly due to the plane configuration of Cz providing more steric hindrance than the line configuration of an alkoxy or alkyl group. In addition, the E_T of CzPPP being higher than that of dC₈OPPP should also be responsible for the lower K_{qsv} in CzPPP.

The triplet energy transfer from the phosphor to conjugated polymers is mainly governed by their difference in E_T and shielding effect provided by side chains in the polymer and/or ligands in the phosphor. The plot of K_{qsv} versus ΔE_T given in Figure 4 provides an overall picture of the correlation. The linear line given for each quencher (polymer) does not mean an existence of a linear relationship; it is merely given for a visual guide. There are two groups of lines: (a) nonshielding in F3 and P4 and (b) shielding in PPPs. In group (a), the P4 line is underneath the F3 line, which reflects less efficiency in quenching resulting from the higher E_T of the former. The K_{qsv} 's

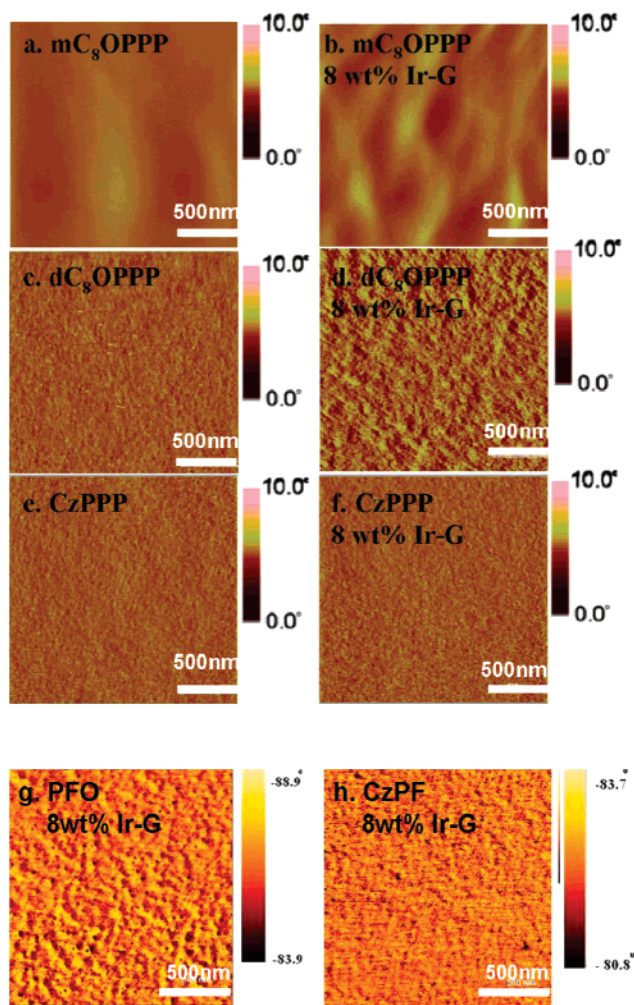


Figure 5. Phase-contrast images of the eight samples: (a) mC₈OPPP, (c) dC₈OPPP and (e) CzPPP, and (b) mC₈OPPP, (d) dC₈OPPP, (f) CzPPP, (g) PFO and (h) CzPF doped with 8 wt % Ir–G, as measured using a scanning probe microscope (from Digital Instrument Nanoscope III).

of PFO and CzPF are located far below the F3 line indicating a possible shielding effect provided by the side chains. In group (b), the three polymers exhibit the following sequence of shielding effect as can be seen from the sequential descending levels: CzPPP > dC₈OPPP > mC₈OPPP.

One further question to be clarified is “Is molecular diffusion in solution a rate-limiting step for the energy transfer process?” If the energy transfer process is molecular diffusion-controlled, the experimental value of K_{qsv} should essentially be invariant for quenchers of widely varying structures; i.e., a mechanical, not a molecular structure, feature is rate-limiting.³¹ However, in our Stern–Volmer experiment, for example, the quenching rate constants of the Ir–B system with mC₈OPPP is larger than that with dC₈OPPP by a factor of 2.4 resulting from the molecular structure difference. Thus the energy transfer is not a molecular diffusion-controlled process.

Improvement in Chemical Compatibility between Host and Guest. Figure 5 shows the scanning probe microscopy (SPM) phase contrast images of pristine polymer films, mC₈OPPP, dC₈OPPP, and CzPPP before and after doping with 8 wt % Ir–G and of PFO and CzPF also doping with 8 wt % Ir–G. Phase separation occurs in the Ir–G doped polymers, and the extents of phase separation for the cases with CzPPP

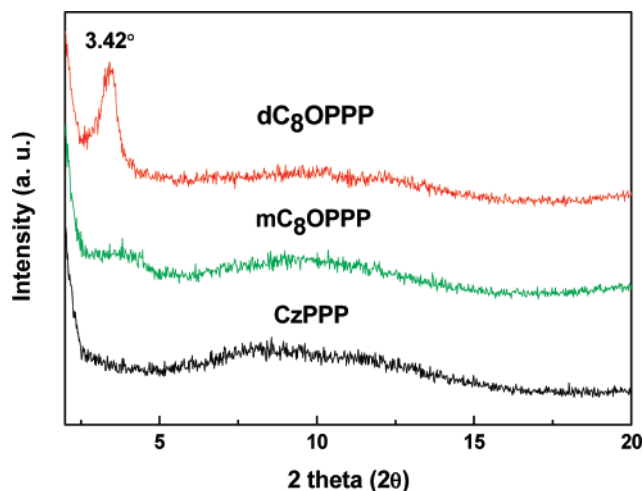


Figure 6. Wide-angle X-ray diffraction patterns of PPPs.

and CzPF are significantly less than those with mC_8OPPP , dC_8OPPP , and PFO. These results indicate that the Cz moiety serves as a compatibilizer between the dopant and polymer. Consequently, CzPPP and CzPF as hosts are expected to allow efficient use of Ir–G (by improved dispersion) upon photoexcitation or electric field excitation.^{3g,9d,15}

WAXD patterns for PPPs are shown in Figure 6. CzPPP is featureless (amorphous and no side chain alignment), while mC_8OPPP is also essentially amorphous but with a very small extent of side chain alignment, as reflected in the presence of a small hump in the 2θ range 3° – 5° . For dC_8OPPP , the side chain alignment is very pronounced as reflected in the presence of an intense and sharp diffraction peak at 3.42° . These results indicate that the Cz moiety prevents an order alignment of the side chain for CzPPP and thus reduces the extent of phase separation of Ir–G from the CzPPP matrix, which is in agreement with the results of AFM studies.

Efficient Green Electrophosphorescence from Ir–G Doped Low E_T Polymers with Dense Side Chains. Figure 7 shows the band diagram of the materials investigated in which the energy levels of CFx,^{12a,b} Ir complexes,^{3b,15a,17} and TPBI^{5b} are taken from previous reports. The HOMO levels of PPPs were measured by cyclic voltammograms (see SI), and the corresponding LUMO levels are deduced from optical band gaps and the HOMO levels. For electroluminescence (EL) studies, dC_8OPPP and CzPPP are chosen as the hosts and Ir–G is chosen as the guest for the bipolar devices (ITO/CFx/polymer: dopant/TPBI/CsF/Ca/Al). The device performances are shown in Figures 8–10, and their characteristic values are listed in Table 2.

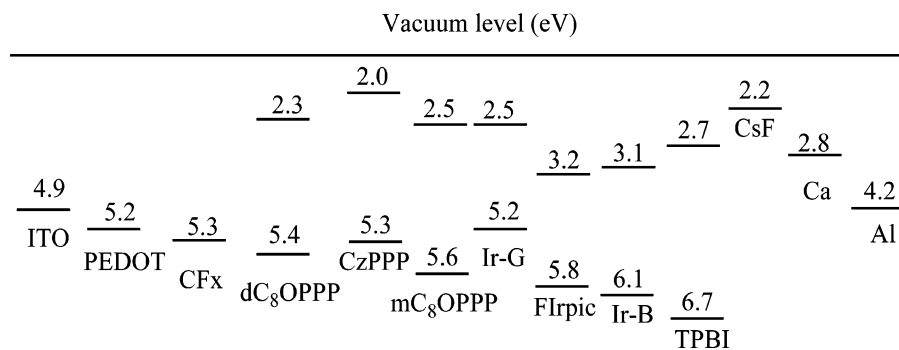


Figure 7. Energy level diagram of the materials used in the devices.

The EL spectra of dC_8OPPP and CzPPP doped with Ir–G (8 wt % for the former and 4–12 wt % for the latter) are all identical to that of the Ir–G emission (peak maximum at 518 nm) (Figure 8). Apparently, singlet excitons formed in the host transfer to the guest, and triplet excitons in the guest must originate from charge trapping in addition to the Förster energy transfer as to be revealed below. As can be seen in Figure 7, the HOMO and LUMO levels of Ir–G lay in between those of the main chain; thus an occurrence of charge trapping upon the electric field excitation can be expected. In addition, the trace host emission in the PL spectrum for dC_8OPPP doped with 8 wt % Ir–G (Figure 3b) disappears in the corresponding EL spectrum, and the current density of CzPPP is higher than those of CzPPP doped with Ir–G (Figure 9a). These observations show that both energy transfer and charge trapping are the mechanisms responsible for the EL performances. The occurrence of charge trapping is very important for such a host/guest system to obtain high performance. Without this condition, triplet excitons generated directly in the guest will be small in population, and those produced by Dexter energy transfer from the host are significantly suppressed since the opportunity for energy transfer is very low due to shielding by side chains. Besides, it has been demonstrated in recent work^{4c} that a resonant and remote intermolecular heavy-atom effect that increases the intersystem crossing rate in the polymer host was found to occur in the Ir-SC4 (a substituted derivative of Ir-(ppy)₃ with increased solubility) doped polyspirobifluorene system. The overlap between the emission spectrum of polyspirobifluorene and MLCT absorption bands of Ir-SC4 is an important factor giving rise to this remote heavy-atom effect. In addition, the wavefunction overlap of delocalized pi electron orbitals between the polymer and aromatic ligands of the complex is another important factor. This mechanism can lead to an increase in the number of host triplet excitons, independent of host E_T ; quenching up to 95% of all singlet excitons and competing effectively with Förster energy transfer are observed. Consequently, devices of Irpic and Ir–B doped PPPs are expected to be poor in performance due to the lack of energy levels matching for hosts and guests (Figure 7). However, the charges (holes and electrons) transporting from host to guest would not be shielded by the dense side chains due to the field dependence of charge transport and lower energy levels of Ir–G. The distance of the fully extended side chain $-O-(CH_2)_{10}-Cz$ is estimated to be about 20 Å (from the oxygen atom to the hydrogen atom bound to carbazole unit at 3 or 6 position), which is within the charge hopping distance (21 Å), as was observed in the molecularly doped polymers¹⁸ (such as 5% triphenylamine

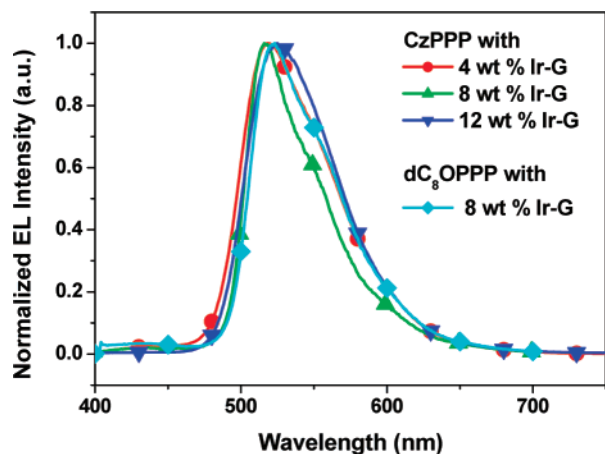


Figure 8. EL spectra of thin films of CzPPP with different Ir-G doping levels and EL spectrum of dC₈OPPP doped with 8 wt % Ir-G.

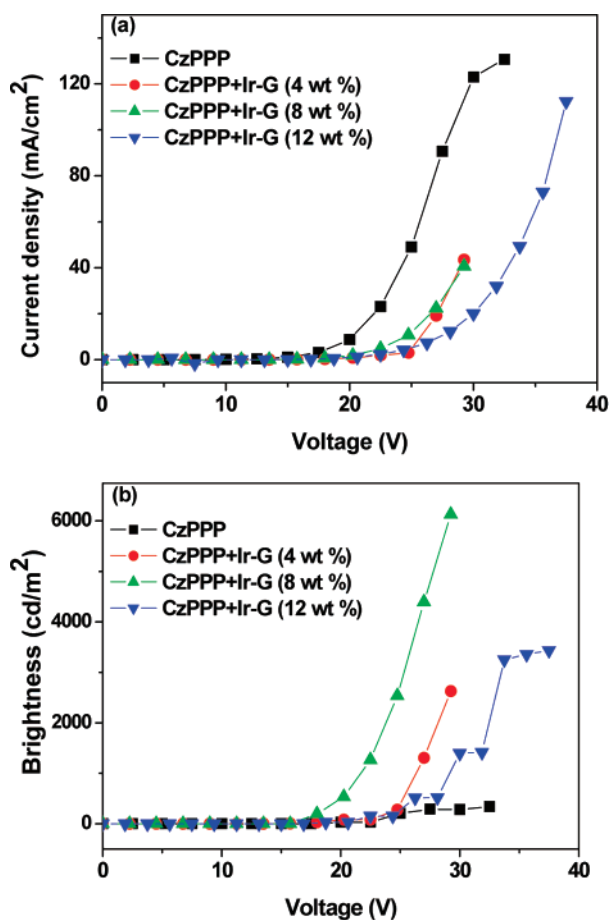


Figure 9. (a) Current density and (b) brightness versus voltage for the devices of Cz-PPP with or without Ir-G doping.

in poly(styrene)^{18c}. Consequently, charge hopping from the host to the guest is expected to take place.

The performances of the bipolar device with 8 wt % Ir-G doped CzPPP give a maximum brightness of 6127 cd/m² and

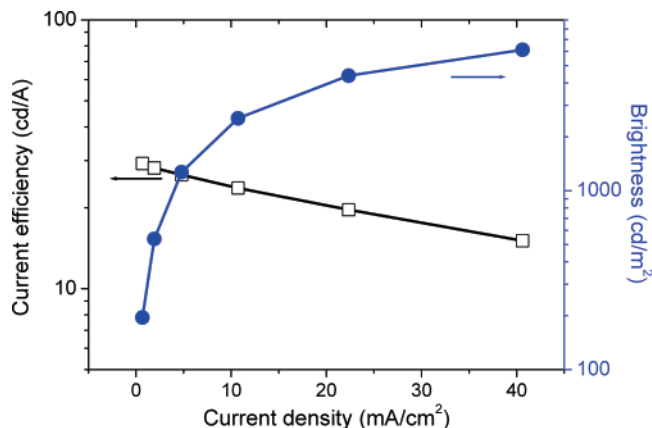


Figure 10. Current efficiency and brightness versus current density for 8 wt % Ir-G doped CzPPP devices.

Table 2. Performances of the Devices^a

host polymer	dopant ^b concn (wt %)	turn-on voltage (V)	max. efficiency η (cd/A) [η_{ext} , %]	max. brightness B_{max} (cd/m ²)
CzPPP	4 (Ir-G)	13	10 [2.8]	2600
	8 (Ir-G)	13	30 [8.25]	6127
	12 (Ir-G)	14	7 [1.87]	4663
dC ₈ OPPP	8 (Ir-G)	16	15 [4.12]	1500

^a ITO/CF_x (2 nm)/emitting polymer layer (100 nm)/TPBI (30 nm)/CsF (1 nm)/Ca (5 nm)/Al. ^b Ir-G: (bis(2-phenylpyridinato-N,C^{2'})iridium(aceetylacetonate).

maximum luminous efficiency of 30 cd/A (corresponding to external quantum efficiency 8.25%) (Table 2). The efficiency of 30 cd/A is higher than those of high E_T polymers as hosts,⁵ but it drops to half (15 cd/A, 4.12%) under the higher current density 40 mA/cm² (Figure 10) which is lower than the efficiency reported by van Dijken et al.^{5a} where the efficiency of 23 cd/A is stable over a large current range up to 46 mA/cm². The 8 wt % doping level gives optimal performance in the range 4–12 wt % as can be seen from the data in Table 2 which were calculated from the curves in Figure 9. For 8 wt % Ir-G doped dC₈OPPP, the performances give a maximum brightness of 1500 cd/m² and maximum luminous efficiency of 15 cd/A (4.12%). As can be seen in Figure 7, despite the uses of CF_x and CsF/Ca/Al for reducing the injection barriers, the turn-on voltages are still high (13–16 V) and the brightness is only modest for both devices. [The work function of CF_x (5.3–5.7 eV) deposited on the ITO surface can be finely tuned by using different rf power (20–50 W) during the plasma polymerization,^{12b} and the CF_x with a work function of 5.3 eV and thickness 2 nm was obtained by using 50 W rf power. The use of a multilayer CsF/Ca/Al cathode was found to be effective for electron injection since CsF can be reduced to form low work function cesium (2.2 eV) by the Ca layer.¹⁹] This is mainly due to the low charge mobilities of PPPs^{9a,b,20} and thus low current densities (Figure 9a). The promoted efficiency of the

(17) D'Andrade, B. W.; Brooks, J.; Adamovich, V.; Thompson, M. E.; Forrest, S. R. *Adv. Mater.* **2002**, *14*, 1032–1036.

(18) (a) Borsenberger, P. M. *J. Appl. Phys.* **1992**, *72*, 5283–5287. (b) Borsenberger, P. M.; Magin, E. H.; Fitzgerald, J. J. *J. Phys. Chem.* **1993**, *97*, 9213–9216. (c) Borsenberger, P. M.; Oregan, M. B. *Chem. Phys.* **1995**, *200*, 257–263. (d) Borsenberger, P. M.; Magin, E. H.; Oregan, M. B.; Sinicropi, J. A. *J. Polym. Sci., Part B: Polym. Phys.* **1996**, *34*, 317–323. (e) Borsenberger, P. M.; Magin, E. H.; Sinicropi, J. A.; Lin, L. B. *Jpn. J. Appl. Phys. Part 1* **1998**, *37*, 166–170.

(19) (a) Greczynski, G.; Fahlman, M.; Salaneck, W. R. *J. Chem. Phys.* **2001**, *114*, 8628–8636. (b) Fung, M. K.; Lai, S. L.; Bao, S. N.; Lee, C. S.; Lee, S. T.; Wu, W. W.; Inbasekaran, M.; O'Brien, J. J. *J. Vac. Sci. Technol. A* **2002**, *20*, 911–918. (c) Brown, T. M.; Friend, R. H.; Millard, I. S.; Lacey, D. J.; Butler, T.; Burroughes, J. H.; Cacialli, F. *J. Appl. Phys.* **2003**, *93*, 6159–6172.

(20) (a) Yang, Y.; Pei, Q.; Heeger, A. J. *J. Appl. Phys.* **1996**, *79*, 934–939. (b) Huang, J. S.; Zhang, H. F.; Tian, W. J.; Hou, J. Y.; Ma, Y. G.; Shen, J. C.; Liu, S. Y. *Synth. Met.* **1997**, *87*, 105–108. (c) Ma, D. G.; Hummelgen, I. A.; Li, R. W. C.; Gruber, J. *J. Phys. D: Appl. Phys.* **2000**, *33*, 1376–1379.

CzPPP-device over the dC₈OPPP-device can be attributed to the better chemical compatibility between the host and guest provided by the incorporation of Cz (Figure 5). In addition, incorporation of 8 wt % Ir–G into the polymers leading to reduction of charge injection barriers (Figure 7) and promoted charge balance within emissive layer could also be the reason for the improved performance in Ir–G doped CzPPP.²¹

Conclusions and Significance

In summary, we found that the dialkoxyl side chains provide effective shielding for the backbone in PPPs such that energy transfer of a triplet exciton from a phosphor dopant (Ir complex) is significantly reduced or almost completely prevented. The shielding effect is more obvious when the E_T of the host is far lower than that of the guest. Moreover, incorporation of Cz on the end of the alkoxyl side chain can further hinder the back triplet energy transfer and enhance chemical compatibility

between host and guest. If the HOMO and LUMO levels of the phosphor dopant are intercalated in those of the host polymer so that charge trapping can occur, the host/guest system is able to emit light solely from the guest efficiently even though the E_T of the host is lower than that of the guest. This observation suggests that the E_T of polymer host is not necessary to be higher than that of phosphor guest for efficient electrophosphorescence. Such a finding provides more freedom for molecular design of electroluminescent polymers as hosts for phosphor dopants.

Acknowledgment. We thank the Ministry of Education (Project 91E-FA04-2-4A) and the National Science Council (Project 95E-2752-E007-005 and 008-PAE) for financial support.

Supporting Information Available: Instrumental, synthesis, device fabrication, optical measurement, Stern–Volmer analysis, AFM, and WXR (PDF). This material is available free of charge via the Internet at <http://pubs.acs.org>.

- (21) (a) Al Attar, H. A.; Monkman, A. P. *Adv. Funct. Mater.* **2006**, *16*, 2231–2242. (b) Matsusue, N.; Ikame, S.; Suzuki, Y.; Naito, H. *Appl. Phys. Lett.* **2004**, *85*, 4046–4048. (c) Matsusue, N.; Suzuki, Y.; Naito, H. *Jpn. J. Appl. Phys. Part 1* **2005**, *44*, 3691–3694.

JA076413I